Otero Fumega, Adolfo; Lado, Jose

Nature of the Unconventional Heavy-Fermion Kondo State in Monolayer CeSiI

Published in:
Nano Letters

DOI:
10.1021/acs.nanolett.4c00619

Published: 10/04/2024

Document Version
Publisher's PDF, also known as Version of record

NANO LETTERS

pubs.acs.org/NanoLett
Letter

Nature of the Unconventional Heavy-Fermion Kondo State in Monolayer CeSiI

Adolfo O. Fumega* and Jose L. Lado*

Cite This: *Nano Lett.* 2024, 24, 4272−4278

Read Online

ACCESS | Metrics & More | Article Recommendations | Supporting Information

ABSTRACT: CeSiI has been recently isolated in the ultrathin limit, establishing CeSiI as the first intrinsic two-dimensional van der Waals heavy-fermion material up to 85 K. We show that, due to the strong spin−orbit coupling, the local moments develop a multipolar real-space magnetic texture, leading to local pseudospins with a nearly vanishing net moment. To elucidate its Kondo-screened regime, we extract from first-principles the parameters of the Kondo lattice model describing this material. We develop a pseudofermion methodology in combination with ab initio calculations to reveal the nature of the heavy-fermion state in CeSiI. We analyze the competing magnetic interactions leading to an unconventional heavy-fermion order as a function of the magnetic exchange between the localized f-electrons and the strength of the Kondo coupling. Our results show that the magnetic exchange interactions promote an unconventional momentum-dependent Kondo-screened phase, establishing the nature of the heavy-fermion state observed in CeSiI.

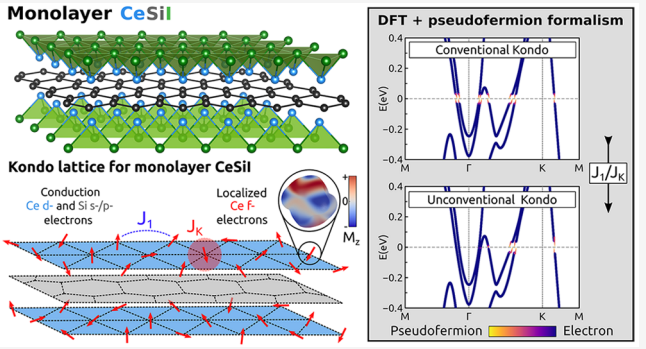

KEYWORDS: *van der Waals materials, heavy-fermion materials, Kondo lattice, ab initio methods, quantum magnetism, 2D materials*

The coexistence of electronic orders in two-dimensional (2D) materials establishes a rich platform for the emergence of new physics. Since the isolation of van der Waals monolayers, a variety of magnetic orders have been observed in the 2D limit, including ferromagnetic,[1,2] quantum spin-liquid candidates,[3,4] and multiferroic order.[5,6] Furthermore, exploring the unique degrees of freedom of van der Waals materials, namely, the easy and clean stacking of layers forming heterostructures and introducing twist angles between layers, has allowed the emergence of new magnetic orders, including orbital ferromagnets[7,8] and heavy-fermion Kondo lattice materials.[9−16] The recent isolation of CeSiI[17] in the ultrathin limit establishes heavy-fermion Kondo insulators as a new member in the family of van der Waals building blocks.

Heavy-fermion systems emerge due to the coexistence of a magnetic lattice that is coupled to a nearly free 2D electron gas forming what is known as a Kondo lattice.[18] Traditionally, these two ingredients have been found in bulk rare-earth compounds, which bring together magnetic moments from the localized f-orbitals and an electron gas from the delocalized orbitals.[19] These Kondo systems display intriguing phase diagrams in which unconventional superconductivity, quantum critical phases, or the already-mentioned heavy-fermion order have been reported.[18,20] Therefore, identifying new heavy-fermion systems is proven to be a powerful strategy for studying novel exotic phenomena.

In the realm of van der Waals materials, heavy-fermion systems have been artificially engineered in heterostructures with different 2D materials including 1T−1H TaS_2 bilayers, $MoTe_2/WSe_2$ bilayers, and MoS_2 bilayers.[9,12,15] Now, monolayer CeSiI brings Kondo physics to a single van der Waals block, allowing us to study these systems from a novel perspective combining typical surface-science experimental techniques such as scanning tunneling microscopy[21] and exploiting the degrees of freedom characteristic of van der Waals materials.[22] However, theoretical studies on monolayer CeSiI are still scarce[14] due to the difficult treatment of Kondo systems from an *ab initio* perspective. This obstacle hinders the study of the complex phase diagram that could arise in CeSiI van der Waals heterostructures.

In this work, we analyze the emergent heavy-fermion phase in monolayer CeSiI. We introduce a formalism based on density functional theory (DFT) calculations combined with an auxiliary pseudofermion variational method. This approach that we termed DFT+pseudofermion allows us to study the heavy-fermion order emerging in this compound. We show that the strong spin−orbit coupling effects lead to an exotic magnetic texture in the local Ce moments, leading to an emergent

Received: February 3, 2024
Revised: February 14, 2024
Accepted: February 15, 2024
Published: February 23, 2024

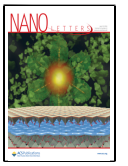

pseudospin Kondo lattice. Using the DFT+pseudofermion formalism, we capture the first-principles multiorbital electronic structure together with the many-body Kondo screening that occurs in CeSiI. In particular, we establish that the competition between the Kondo coupling and the magnetic exchange interactions between the localized Ce f-electrons gives rise to the unconventional nodal heavy-fermion order that can be proved experimentally.

It is instructive to start analyzing the electronic structure of the monolayer CeSiI arising directly from DFT. The structure of monolayer CeSiI is shown in Figure 1a, where two triangular

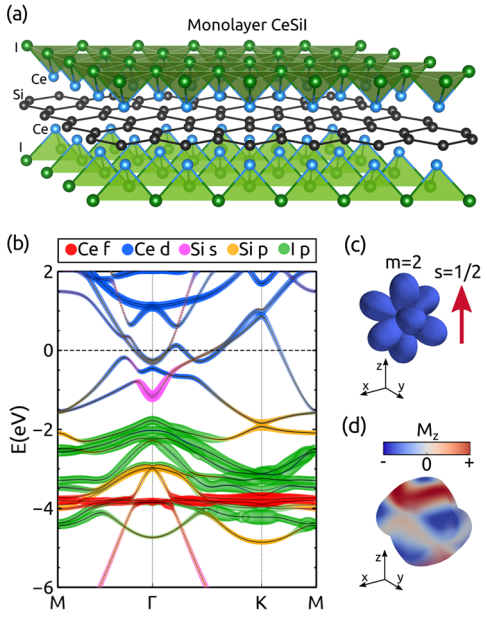

Figure 1. (a) Structure of monolayer CeSiI. (b) DFT orbital-resolved band structure of CeSiI, enforcing a symmetry-broken ferromagnetic arrangement of the Ce magnetic moments. Panels c and d show the magnetization of the occupied f-state in the absence (c) and presence (d) of spin−orbit coupling. In the latter case, the net magnetization of the occupied orbital is quenched, leading to a microscopic spin texture in the occupied state.

lattices of Ce and I atoms encapsulate a staggered honeycomb lattice of Si atoms, forming the single van der Waals block. Figure 1b shows the orbital-resolved band structure of monolayer CeSiI obtained from DFT calculations using the LDA+U formalism, enforcing a symmetry-broken ferromagnetic arrangement and including spin−orbit coupling (SOC), with U corresponding to the on-site Coulomb interaction of the localized Ce f-electrons. In the plot, U = 8 eV was considered for the f-electrons. However, the results and discussion presented here are not qualitatively affected by the election of a different U in the strongly localized limit. The strong electron−electron interactions in the f-orbitals of Ce give rise to the formation of a local magnetic moment, leading to a set of deep occupied nearly dispersionless flat bands (shown in red in Figure 1b). The electrons belonging to Si sp-orbitals and Ce d-orbitals are in comparison strongly dispersive, leading to a metallic behavior (shown in pink, yellow, and blue, respectively, in Figure 1b). These conduction states show strong hybridization between the different elements. Enforcing a ferromagnetic arrangement between the f-electrons is a technical consideration that allows a simpler treatment in the single unit cell and has no major effect on the analysis of the orbital character of the bands.

A key feature of this material is the existence of very strong spin−orbit coupling. This strong spin−orbit coupling has a major effect on the local moment of the f-orbitals. In the absence of spin−orbit coupling, the f-electrons display an orbital momentum m = 2 and spin 1/2 (Figure 1c). However, when spin−orbit interactions are included, the original net S = 1/2 moment transforms into a complex spin structure in the f-manifold, with a quenched net magnetic moment (Figure 1d). This orbital degeneracy together with strong spin−orbit coupling effects can give rise to a hidden magnetic order,[23−28] characterized by a multipolar localized spin texture with a quenched magnetic moment that is difficult to identify in experiments. From an effective model point of view, the unpaired electron behaves as a pseudospin 1/2, which is the required feature for the emergence of heavy-fermion phenomena, and monolayer CeSiI stems from the Kondo lattice Hamiltonian[29,30]

$$H = \sum_{ij} t_{ij} c_i^{\dagger} c_j + \sum_{\langle i,\alpha \rangle} J_K \vec{S}_\alpha \cdot \vec{\sigma}_{s,s'} c_{i,s}^{\dagger} c_{i,s'} + J_1 \sum_{\langle \alpha,\beta \rangle} \vec{S}_\alpha \cdot \vec{S}_\beta \quad (1)$$

where $c_i^{\dagger}$ is the creation operator for Wannier conduction band electrons, t_{ij} corresponds to their hopping energy, $\langle\ \rangle$ denotes first neighbors, J_1 is the exchange coupling between first-neighbor pseudospin sites of the f-electrons, and J_K is the Kondo coupling between the localized pseudospins and the conduction electrons. It is important to note that in the Kondo problem these pseudospins act as a real spin 1/2, since the Hilbert subspace representation of these pseudospins corresponds to one of spins 1/2 despite the local magnetic texture that they might display. Therefore, the J_1 interaction captures the magnetic exchange interaction between these pseudospins. The schematic of this model is shown in Figure 2a. The previous Hamiltonian realizes a Kondo lattice model, whose physics is controlled by two main parameters. The exchange coupling J_1 promotes magnetic ordering in the magnetic lattice formed by the f-electrons. In contrast, the Kondo coupling J_K promotes the screening of each spin site, by forming a singlet with a conduction electron of the conduction gas.[30] This screening of spin sites in the lattice creates a coherent set of scattering centers, leading to the appearance of a heavy-fermion gap.[31] The competition between those two energy scales dominates the physics of a heavy-fermion monolayer.

Traditional DFT calculations cannot directly capture the many-body heavy-fermion behavior in the electronic structure. However, they can be used to provide an estimate of the competing parameters entering the Kondo lattice Hamiltonian. Specifically, the exchange coupling can be extracted by comparing the energies of different magnetic arrangements (Figure 2b). It is important to point out that the exchange coupling J_1 can have both direct and indirect exchange through the I atoms and an indirect interaction mediated by the electron gas. This last interaction, known as the RKKY interaction, is the dominant one due to the strongly localized f-electrons residing within the electron gas. First principle methods incorporate all the contributions, and therefore, the exchange extracted represents the net one. On the other hand, the Kondo coupling stems from the induced spin splitting in the conduction bath by the local magnetic moment. Therefore, J_K can be estimated as the energy shift in the density of states (DOS) of the conduction bands at the Fermi level (Figure 2c). The DFT+U estimation of J_1 and J_K is shown in Figure 2d and e, respectively. We can observe a robust *ab initio* estimation of these quantities; i.e., they are shown to be independent of the onsite Coulomb interaction

https://doi.org/10.1021/acs.nanolett.4c00619
Nano Lett. 2024, 24, 4272−4278

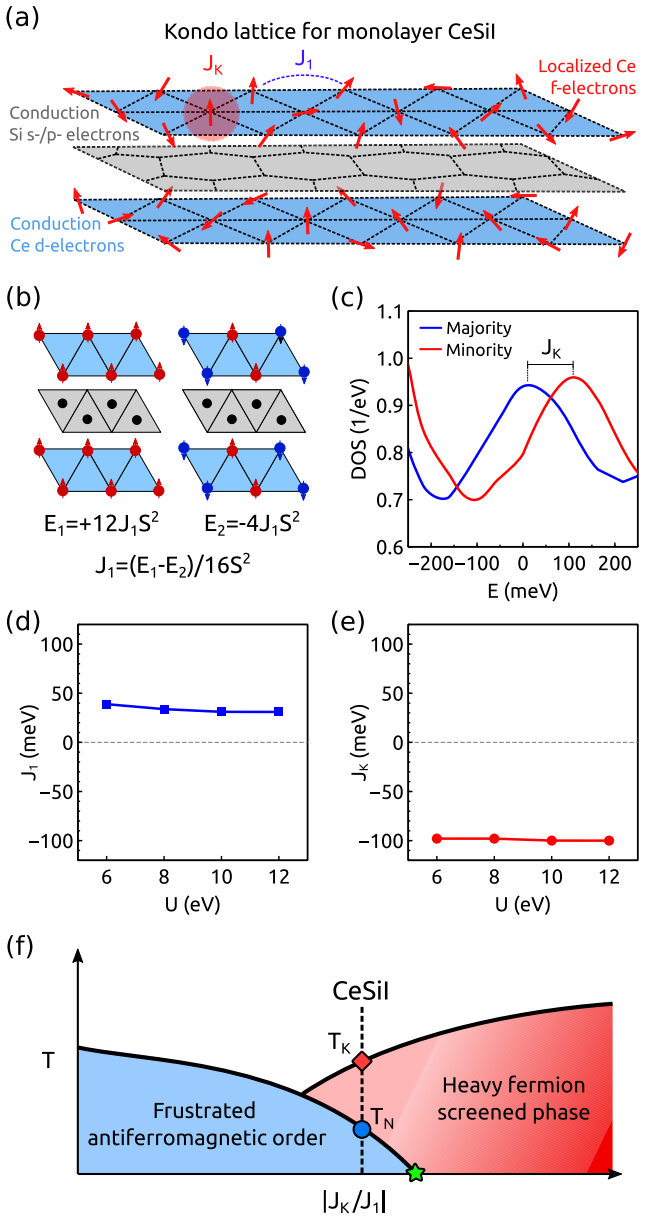

Figure 2. (a) Schematic low-energy model for CeSiI. The spin−lattice stems from the localized f-electrons of Ce, while the conduction electrons correspond mainly to the d-electrons of Ce. First-neighbor spins are coupled via a magnetic exchange interaction J_1, and Kondo is coupled to the conduction electrons with J_K. (b) Magnetic configurations used to estimate J_1. (c) Spin-polarized density of states plot used to estimate J_K. Evolution of J_1 (d) and J_K (e) from DFT+U as a function of the Coulomb interaction U of the f-orbitals. (f) Schematic phase diagram of the Kondo lattice model, where CeSiI is found to enter into a heavy-fermion phase below T_K and an anti-ferromagnetic one below T_N. The green asterisk denotes the quantum critical region.

of the f-electrons U. An anti-ferromagnetic J_1 is obtained in good agreement with magnetometry measurements[32] which suggests that the phase diagram of the competing J_K−J_1 triangular Kondo lattice (eq 1) would display a quantum critical phase between a frustrated magnetic order and the heavy-fermion order,[33−37] instead of the usual quantum critical point between a ferromagnetic and heavy-fermion order (Figure 2d). DFT+U provides an estimation of $J_1 \simeq 30$ meV and $J_K \simeq -100$ meV, which suggests that monolayer CeSiI can enter the heavy-fermion phase dominated by J_K, but with a non-negligible magnetic exchange J_1 between the f-electrons. This finite J_1 exchange promotes the formation of a frustrated magnetic order at the lowest temperature below 7.5 K, with screening from Kondo physics dominating between 7.5 and 85 K[17] as represented in Figure 2f.

The screened coherent heavy-fermion Kondo regime[17] can be directly accounted by the Kondo lattice model. The previous Kondo lattice model can be solved using an auxiliary fermion (pseudofermion or parton) formalism for Kondo sites[38−43] $\vec{S}_\alpha = \frac{1}{2}\sum_{s,s'} \sigma_{s,s} f^\dagger_{s,\alpha} f_{s',\alpha}$ with the Fock constraint $\sum_s f^\dagger_{s,\alpha} f_{s',\alpha} = 1$. By replacement of spin operators by auxiliary fermions, the Hamiltonian becomes biquadratic in field operators. We can perform a decoupling of the biquadratic term by introducing the Kondo hybridization functions, leading to the following effective Hamiltonian

$$H = \sum_{\nu,\mathbf{k}} \epsilon_\nu(\mathbf{k}) c^\dagger_{\mathbf{k},\nu} c_{\mathbf{k},\nu} + \sum_{\alpha,\mathbf{k}} \gamma_1(\mathbf{k}) f^\dagger_{\mathbf{k},\alpha} f_{\mathbf{k},\alpha} + \sum_{\nu,\alpha,\mathbf{k}} \gamma_K^{\nu,\alpha}(\mathbf{k}) f^\dagger_{\mathbf{k},\alpha} c_{\mathbf{k},\nu} \quad (2)$$

where $f^\dagger_{\alpha,s}$ are the pseudofermion creation operators in reciprocal space. The Kondo hybridization function depends on the Kondo coupling as $\gamma_K(\mathbf{k}) \sim J_K\langle c^\dagger_{\mathbf{k}} f_{\mathbf{k}}\rangle$, and the dispersion of the pseudofermions is given by the Fourier transform of the pseudofermion mean-field $|\gamma_1(\mathbf{k})| \sim J_1$. This Hamiltonian can be solved in combination with first-principles electronic calculations for monolayer CeSiI. A DFT+pseudofermion formalism can be established by expanding the Hilbert space of the DFT states (first term in eq 2) to include the pseudofermions (second term in eq 2) and their hybridization with the DFT states (third term in eq 2). This allows us to compute the electronic structure of monolayer CeSiI in the presence of Kondo screening. Since the unit cell of monolayer CeSiI has two Ce atoms that give rise to two localized pseudospins 1/2, four pseudofermions are considered in this DFT+pseudofermion formalism. In the case of two 1/2-real spins, one would also consider four pseudofermions in the DFT+pseudofermion formalism. The pseudospins are a result of the spin−orbit coupling leading to a complex spin texture. Two channels in each pseudofermion do not correspond to up and down but the two channels of a Kramers pair. Specifically, the two channels of a Kramers pair have the property that one channel is the time reversal of the other. These two channels are analogous to the two degrees of freedom of an electronic structure featuring strong spin−orbit coupling effects, where the spin degeneracy is associated with two Kramers pairs instead of two pure spin channels. Therefore, both have the same technical implementation in our formalism. The hybridization function γ_K is in general momentum-, frequency-, and band-dependent. The frequency and band dependence is incorporated with an ansatz promoting hybridization with the closest four bands to the Fermi energy including a frequency-dependent envelope $e^{-(\epsilon_\nu(\mathbf{k})-E_F)^2/J_K^2}$, that accounts for the decreased hybridization away from the chemical potential E_F.

The results for the calculations of monolayer CeSiI in the DFT+pseudofermion formalism in the non-magnetic Kondo screened regime are summarized in Figure 3. In the absence of Kondo hybridization $\gamma_K(\mathbf{k}) = 0$, the DFT band structure (Figure 3a) shows a complex Fermi surface with different pockets around the Γ and K points (Figure 3b). When the Kondo hybridization is finite $\gamma_K(\mathbf{k}) \neq 0$, gaps appear in the electronic

https://doi.org/10.1021/acs.nanolett.4c00619
Nano Lett. 2024, 24, 4272−4278

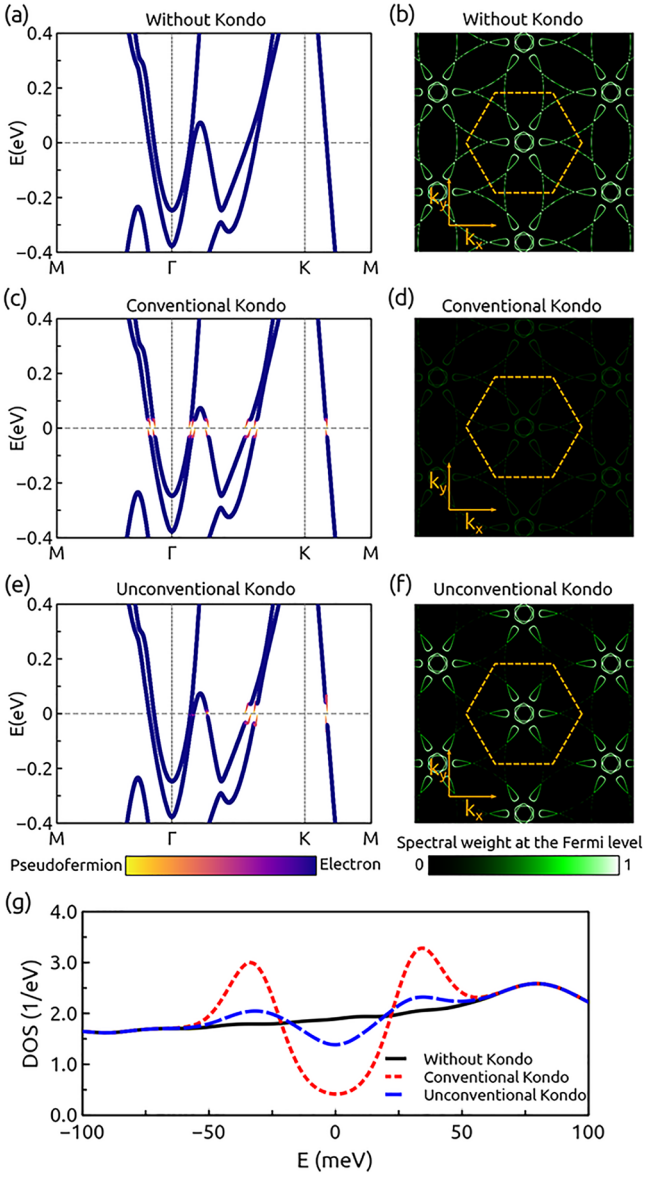

Figure 3. Electronic structure without Kondo hybridization (a, b), with conventional Kondo hybridization (b, c), and with unconventional nodal heavy-fermion hybridization (d, e). Panels a, c, and e show the momentum-resolved spectral function, and panels b, d, and f show the Fermi surface reconstruction. (g) Spectral function observed showing the differences between conventional and unconventional nodal hybridization.

structure at the Fermi energy. From a symmetry point of view, two solutions can emerge when solving the variational Hamiltonian of eq 2: (i) a conventional s-wave Kondo hybridization opening a gap in the whole Fermi surface (Figure 3c,d) and with a U-shaped gapped spectral function (Figure 3g) or (ii) an unconventional nodal f-wave Kondo hybridization opening gaps only around the K points in the Fermi surface (Figures 3e,f) and displaying a V-shaped spectral function (Figure 3g). This gapless heavy-fermion behavior produces a decreased slope of the band structure (effective electron mass enhancement) mostly around the K points. This kind of momentum dependence of the Kondo hybridization has already been experimentally observed and analyzed in other heavy-fermion compounds[44] and in particular Ce-based systems.[45−50] As in the case of CeSiI, they show a *k*-dependent Kondo hybridization. However, these compounds have a non-van der Waals tetragonal structure. Therefore, their nodal behavior displays a different symmetry than the one observed in the triangular lattice of CeSiI. This would have implications in the symmetry of the superconducting order parameters that might occur in the phase diagram of these heavy-fermion systems.[51] The nodal behavior could be detected via ARPES experiments as previously done for the other Ce-based compounds or using a scanning tunneling microscope as it has already been used to test unconventional nodal superconductors.[52,53]

The previous classification focused on the case where the Kondo pseudofermions are dispersionless, which is equivalent to considering vanishingly small exchange coupling between magnetic sites, i.e., $\gamma_1(\mathbf{k}) = 0$ in eq 2. Due to the finite exchange J_1, the Kondo pseudofermions will develop a finite dispersion ($\gamma_1(\mathbf{k}) \neq 0$). In the limit of $J_1 \gg J_K$ the system will develop magnetic order. Here we will focus on the case $J_1 \neq 0$, but below, the quantum phase transition to the magnetically ordered regime. The calculations of the electronic structure with the DFT+pseudofermion formalism are shown in Figure 4, now considering the dispersion in the Kondo spinons. As a reference, we show first how the composite spectra look in the presence of spinon dispersion but vanishing Kondo hybridization in Figure 4a−d for different values of $\gamma_1(\mathbf{k})$. While this situation is not physically observable due to the requirement of Kondo screening to reach the spinon representation, it provides a useful starting point to rationalize the effect of $\gamma_1(\mathbf{k})$ on the conduction gas. The pseudofermion dispersion makes the spinon modes off-resonant with the Fermi surface in major parts of the reciprocal space. This effect implies that, once the Kondo hybridization is included as shown in Figure 4e−h, the gap opening at the Fermi surface becomes much less pronounced, keeping certain parts of the electronic structure gapless. The dispersive pseudofermion band is closer to the Fermi level and more flat around the K points than around the Γ point. Considering that the Kondo hybridization is energy-dependent, i.e., the closer to the Fermi level the pseudofermion energy, the stronger the hybridization, this leads to a stronger gap around the K points than in the electronic bands around Γ. This gapless electronic structure emerges in the presence of a conventional s-wave Kondo hybridization, emulating an unconventional nodal spectrum. The previous phenomenology shows that the exchange between magnetic sites leads to a weakening of the heavy-fermion gap. In particular, it can be observed that increasing the γ_1/γ_K ratio promotes unconventional nodal Kondo hybridization. The multiorbital character, meaning having several bands crossing the Fermi level, provides a complex Fermi surface with pockets around the Γ and K points (Figure 3b). In the presence of Kondo hybridization, the magnetic exchange interactions promote the formation of the Kondo gap around the K points. DMFT calculations have been performed on CeSiI.[14] In this analysis, a conventional Kondo peak is captured for this system. To study an unconventional nodal behavior within a DMFT methodology, a local dependency in the self-energy could be included. This would introduce in the DMFT calculations the nodal effect that we are capturing by the pseudofermion dispersion within our auxiliary fermion mean-field theory combined with DFT. Apart from that, the Kondo hybridizations occurring slightly away from the Fermi level that have been experimentally reported[17] are accounted for by the DFT+pseudofermion formalism in contrast to the DMFT methodology. Finally, it is worth noting that, below the magnetic transition temperature 7.5 K, the previous non-magnetic fully

https://doi.org/10.1021/acs.nanolett.4c00619
Nano Lett. 2024, 24, 4272−4278

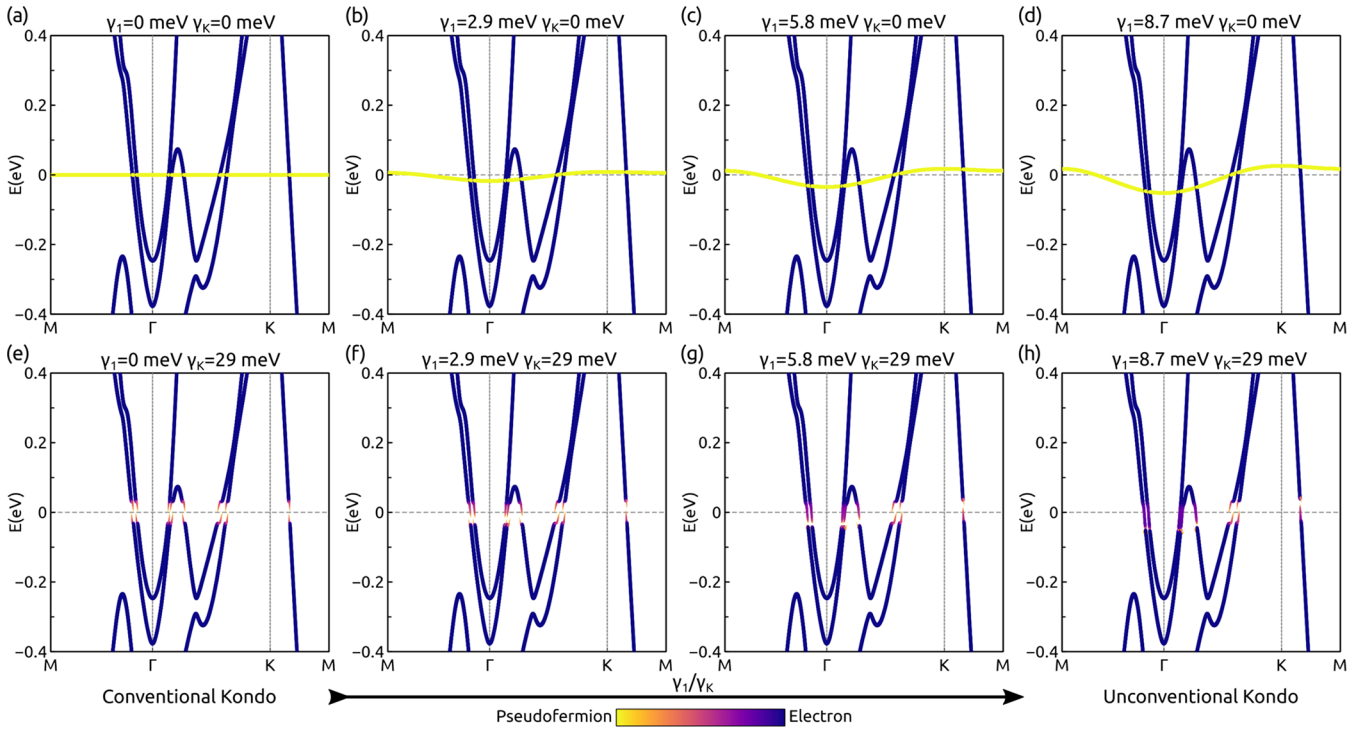

Figure 4. Electron-pseudofermion dispersion in the presence of a sizable exchange coupling J_1 between Kondo sites. Panels a−d show the decoupled pseudofermion and electronic structures as a reference. Panels e−h show the composite electronic structure in the presence of Kondo hybridization, showing that the increase of an exchange coupling and associated pseudofermion dispersion leads to a soft heavy-fermion gap.

screened regime gives rise to a spin-polarized state featuring Kondo correlations, and its treatment requires including finite magnetic ordering in the pseudofermion formalism.

The 2D nature of this material provides promising strategies to tune the ground state. Strain in the monolayer would allow controlling the ratio between J_K/J_1, allowing us to tune the unconventional nature of the heavy-fermion order or to push the system toward a quantum phase transition to a magnetically ordered state (Figure 2f). In particular, strain can allow the ratio J_K/J_1 to be shifted, drifting the system to the heavy-fermion regime at $T = 0$ and completely suppressing magnetic ordering even below 7.5 K. Interestingly, strain will also impact the local crystal field in the Ce atoms, potentially leading to orbital transition in the local magnetic sites. The frustrated nature of the underlying magnetic lattice makes the system ideal to explore the interplay between quantum magnetism and heavy-fermion physics. Furthermore, its monolayer limit will potentially allow tuning this heavy-fermion material directly with a gate, allowing the Kondo lattice to be doped and drifting the system toward a hidden order or unconventional superconducting state[54] as observed in other heavy-fermion compounds.

To summarize, we have presented the microscopic analysis of the heavy-fermion state in the van der Waals monolayer CeSiI. Using first-principles methods, we established the existence of local moments in Ce realizing a multipolar internal magnetic texture with a vanishingly small local moment. These results show that strong spin−orbit coupling effects render this system into a Kondo lattice system with pseudospin 1/2. Our first-principles methods allow us to extract the relevant energy scales of the Kondo lattice model, including the exchange coupling between the localized moments and the Kondo coupling. We introduce a DFT+pseudofermion formalism that combines first-principles calculations with a parton pseudofermion methodology, allowing us to directly compute the multiorbital heavy-fermion electronic structure. We showed that the sizable exchange coupling between moments together with the multiband nature of this system leads to a momentum-dependent heavy-fermion hybridization in the Kondo screened regime, in comparison with the stronger gap opening in single band heavy-fermion systems. Our results establish the first-principles electronic structure of CeSiI, exemplifying how a combination of density functional theory and pseudofermion formalism allows the modeling of complex heavy-fermion van der Waals materials.

■ ASSOCIATED CONTENT

Supporting Information

The Supporting Information is available free of charge at https://pubs.acs.org/doi/10.1021/acs.nanolett.4c00619.

DFT electronic band structure of monolayer CeSiI in the absence of spin−orbit coupling and strain dependence of the Kondo lattice parameters (PDF)

■ AUTHOR INFORMATION

Corresponding Authors

Adolfo O. Fumega − *Department of Applied Physics, Aalto University, 02150 Espoo, Finland;* orcid.org/0000-0002-3385-6409; Email: adolfo.oterofumega@aalto.fi

Jose L. Lado − *Department of Applied Physics, Aalto University, 02150 Espoo, Finland;* Email: jose.lado@aalto.fi

Complete contact information is available at: https://pubs.acs.org/10.1021/acs.nanolett.4c00619

Notes

The authors declare no competing financial interest.

https://doi.org/10.1021/acs.nanolett.4c00619
Nano Lett. 2024, 24, 4272−4278

■ ACKNOWLEDGMENTS

We acknowledge the computational resources provided by the Aalto Science-IT project and the financial support from the Academy of Finland (Project Nos. 331342, 336243, and 349696) and the Jane and Aatos Erkko Foundation. We thank A. Pasupathy for useful discussions.

■ REFERENCES

(1) Huang, B.; Clark, G.; Navarro-Moratalla, E.; Klein, D. R.; Cheng, R.; Seyler, K. L.; Zhong, D.; Schmidgall, E.; McGuire, M. A.; Cobden, D. H.; Yao, W.; Xiao, D.; Jarillo-Herrero, P.; Xu, X. Layer-dependent ferromagnetism in a van der Waals crystal down to the monolayer limit. *Nature* **2017**, *546*, 270−273.

(2) Fei, Z.; Huang, B.; Malinowski, P.; Wang, W.; Song, T.; Sanchez, J.; Yao, W.; Xiao, D.; Zhu, X.; May, A. F.; Wu, W.; Cobden, D. H.; Chu, J.-H.; Xu, X. Two-dimensional itinerant ferromagnetism in atomically thin Fe3GeTe2. *Nat. Mater.* **2018**, *17*, 778−782.

(3) Ruan, W.; et al. Evidence for quantum spin liquid behaviour in single-layer 1T-TaSe2 from scanning tunnelling microscopy. *Nat. Phys.* **2021**, *17*, 1154−1161.

(4) Chen, Y.; et al. Evidence for a spinon Kondo effect in cobalt atoms on single-layer 1T-TaSe2. *Nat. Phys.* **2022**, *18*, 1335−1340.

(5) Song, Q.; Occhialini, C. A.; Ergeçen, E.; Ilyas, B.; Amoroso, D.; Barone, P.; Kapeghian, J.; Watanabe, K.; Taniguchi, T.; Botana, A. S.; Picozzi, S.; Gedik, N.; Comin, R. Evidence for a single-layer van der Waals multiferroic. *Nature* **2022**, *602*, 601−605.

(6) Amini, M.; Fumega, A. O.; González-Herrero, H.; Vaňo, V.; Kezilebieke, S.; Lado, J. L.; Liljeroth, P. Atomic-Scale Visualization of Multiferroicity in Monolayer NiI2. *Adv. Mater.* **2024**, No. 2311342.

(7) Serlin, M.; Tschirhart, C. L.; Polshyn, H.; Zhang, Y.; Zhu, J.; Watanabe, K.; Taniguchi, T.; Balents, L.; Young, A. F. Intrinsic quantized anomalous Hall effect in a moiré heterostructure. *Science* **2020**, *367*, 900−903.

(8) Park, H.; et al. Observation of fractionally quantized anomalous Hall effect. *Nature* **2023**, *622*, 74−79.

(9) Vaňo, V.; Amini, M.; Ganguli, S. C.; Chen, G.; Lado, J. L.; Kezilebieke, S.; Liljeroth, P. Artificial heavy fermions in a van der Waals heterostructure. *Nature* **2021**, *599*, 582−586.

(10) Ramires, A.; Lado, J. L. Emulating Heavy Fermions in Twisted Trilayer Graphene. *Phys. Rev. Lett.* **2021**, *127*, No. 026401.

(11) Song, Z.-D.; Bernevig, B. A. Magic-Angle Twisted Bilayer Graphene as a Topological Heavy Fermion Problem. *Phys. Rev. Lett.* **2022**, *129*, No. 047601.

(12) Zhao, W.; Shen, B.; Tao, Z.; Han, Z.; Kang, K.; Watanabe, K.; Taniguchi, T.; Mak, K. F.; Shan, J. Gate-tunable heavy fermions in a moiré Kondo lattice. *Nature* **2023**, *616*, 61−65.

(13) Kumar, A.; Hu, N. C.; MacDonald, A. H.; Potter, A. C. Gate-tunable heavy fermion quantum criticality in a moiré Kondo lattice. *Phys. Rev. B* **2022**, *106*, No. L041116.

(14) Jang, B. G.; Lee, C.; Zhu, J.-X.; Shim, J. H. Exploring two-dimensional van der Waals heavy-fermion material: Data mining theoretical approach. *npj 2D Materials and Applications* **2022**, *6*, 80.

(15) Guerci, D.; Wang, J.; Zang, J.; Cano, J.; Pixley, J. H.; Millis, A. Chiral Kondo lattice in doped $MoTe_2/WSe_2$ bilayers. *Science Advances* **2023**, *9*, 1−7.

(16) Zhao, W.; Shen, B.; Tao, Z.; Kim, S.; Knüppel, P.; Han, Z.; Zhang, Y.; Watanabe, K.; Taniguchi, T.; Chowdhury, D.; Shan, J.; Mak, K. F. Emergence of ferromagnetism at the onset of moiré Kondo breakdown. *arXiv e-prints* 2023, arXiv:2310.06044. DOI: 10.48550/arXiv.2310.06044 (accessed October 11, 2023).

(17) Posey, V. A.; et al. Two-dimensional heavy fermions in the van der Waals metal CeSiI. *Nature* **2024**, *625*, 483−488.

(18) Coleman, P. Heavy Fermions and the Kondo Lattice: a 21st Century Perspective. *arXiv e-prints* 2015, arXiv:1509.05769. DOI: 10.48550/arXiv.1509.05769 (accessed July 11, 2023).

(19) Stewart, G. R. Heavy-fermion systems. *Rev. Mod. Phys.* **1984**, *56*, 755−787.

(20) Si, Q.; Steglich, F. Heavy Fermions and Quantum Phase Transitions. *Science* **2010**, *329*, 1161−1166.

(21) Kirchner, S.; Paschen, S.; Chen, Q.; Wirth, S.; Feng, D.; Thompson, J. D.; Si, Q. Colloquium: Heavy-electron quantum criticality and single-particle spectroscopy. *Rev. Mod. Phys.* **2020**, *92*, No. 011002.

(22) Geim, A. K.; Grigorieva, I. V. Van der Waals heterostructures. *Nature* **2013**, *499*, 419−425.

(23) Cricchio, F.; Bultmark, F.; Grånäs, O.; Nordström, L. Itinerant Magnetic Multipole Moments of Rank Five as the Hidden Order in URu_2Si_2. *Phys. Rev. Lett.* **2009**, *103*, No. 107202.

(24) Nayak, C. Density-wave states of nonzero angular momentum. *Phys. Rev. B* **2000**, *62*, 4880−4889.

(25) Okazaki, R.; Shibauchi, T.; Shi, H. J.; Haga, Y.; Matsuda, T. D.; Yamamoto, E.; Onuki, Y.; Ikeda, H.; Matsuda, Y. Rotational Symmetry Breaking in the Hidden-Order Phase of URu_2Si_2. *Science* **2011**, *331*, 439−442.

(26) Ikeda, H.; Ohashi, Y. Theory of Unconventional Spin Density Wave: A Possible Mechanism of the Micromagnetism in U-based Heavy Fermion Compounds. *Phys. Rev. Lett.* **1998**, *81*, 3723−3726.

(27) Mydosh, J. A.; Oppeneer, P. M. Colloquium: Hidden order, superconductivity, and magnetism: The unsolved case of URu_2Si_2. *Rev. Mod. Phys.* **2011**, *83*, 1301−1322.

(28) Mydosh, J. A.; Oppeneer, P. M.; Riseborough, P. S. Hidden order and beyond: an experimental−theoretical overview of the multifaceted behavior of URu_2Si_2. *J. Phys.: Condens. Matter* **2020**, *32*, No. 143002.

(29) Kasuya, T. A Theory of Metallic Ferro- and Antiferromagnetism on Zener's Model. *Prog. Theor. Phys.* **1956**, *16*, 45−57.

(30) Tsunetsugu, H.; Sigrist, M.; Ueda, K. The ground-state phase diagram of the one-dimensional Kondo lattice model. *Rev. Mod. Phys.* **1997**, *69*, 809−864.

(31) Riseborough, P. S. Heavy fermion semiconductors. *Adv. Phys.* **2000**, *49*, 257−320.

(32) Okuma, R.; Ritter, C.; Nilsen, G. J.; Okada, Y. Magnetic frustration in a van der Waals metal CeSiI. *Phys. Rev. Mater.* **2021**, *5*, No. L121401.

(33) Coleman, P.; Nevidomskyy, A. H. Frustration and the Kondo Effect in Heavy Fermion Materials. *Journal of Low Temperature Physics* **2010**, *161*, 182−202.

(34) Tokiwa, Y.; Stingl, C.; Kim, M.-S.; Takabatake, T.; Gegenwart, P. Characteristic signatures of quantum criticality driven by geometrical frustration. *Science Advances* **2015**, *1*, 1−6.

(35) Zhao, H.; Zhang, J.; Lyu, M.; Bachus, S.; Tokiwa, Y.; Gegenwart, P.; Zhang, S.; Cheng, J.; Yang, Y.-f.; Chen, G.; Isikawa, Y.; Si, Q.; Steglich, F.; Sun, P. Quantum-critical phase from frustrated magnetism in a strongly correlated metal. *Nat. Phys.* **2019**, *15*, 1261−1266.

(36) Ramires, A. Frustration can be critical. *Nat. Phys.* **2019**, *15*, 1212−1214.

(37) Kavai, M.; Friedman, J.; Sherman, K.; Gong, M.; Giannakis, I.; Hajinazar, S.; Hu, H.; Grefe, S. E.; Leshen, J.; Yang, Q.; Nakatsuji, S.; Kolmogorov, A. N.; Si, Q.; Lawler, M.; Aynajian, P. Inhomogeneous Kondo-lattice in geometrically frustrated Pr2Ir2O7. *Nat. Commun.* **2021**, *12*, 1−8.

(38) Coleman, P. New approach to the mixed-valence problem. *Phys. Rev. B* **1984**, *29*, 3035−3044.

(39) Auerbach, A.; Levin, K. Kondo Bosons and the Kondo Lattice: Microscopic Basis for the Heavy Fermi Liquid. *Phys. Rev. Lett.* **1986**, *57*, 877−880.

(40) Millis, A. J.; Lee, P. A. Large-orbital-degeneracy expansion for the lattice Anderson model. *Phys. Rev. B* **1987**, *35*, 3394−3414.

(41) Ramires, A.; Coleman, P. Supersymmetric approach to heavy fermion systems. *Phys. Rev. B* **2016**, *93*, No. 035120.

(42) Ramires, A.; Coleman, P. Theory of the Electron Spin Resonance in the Heavy Fermion Metal β−$YbAlB_4$. *Phys. Rev. Lett.* **2014**, *112*, No. 116405.

(43) Coleman, P. Mixed valence as an almost broken symmetry. *Phys. Rev. B* **1987**, *35*, 5072−5116.

(44) Danzenbächer, S.; et al. Momentum dependence of 4f hybridization in heavy-fermion compounds: Angle-resolved photo-

https://doi.org/10.1021/acs.nanolett.4c00619
Nano Lett. 2024, 24, 4272−4278

emission study of $YbIr_2Si_2$ and $YbRh_2Si_2$. *Phys. Rev. B* **2007**, *75*, No. 045109.
(45) Danzenbächer, S.; Kucherenko, Y.; Heber, M.; Vyalikh, D. V.; Molodtsov, S. L.; Servedio, V. D. P.; Laubschat, C. Wave-vector dependent intensity variations of the Kondo peak in photoemission from $CePd_3$. *Phys. Rev. B* **2005**, *72*, No. 033104.
(46) Koitzsch, A.; Borisenko, S. V.; Inosov, D.; Geck, J.; Zabolotnyy, V. B.; Shiozawa, H.; Knupfer, M.; Fink, J.; Büchner, B.; Bauer, E. D.; Sarrao, J. L.; Follath, R. Hybridization effects in $CeCoIn_5$ observed by angle-resolved photoemission. *Phys. Rev. B* **2008**, *77*, No. 155128.
(47) Fujimori, S.-i.; Fujimori, A.; Shimada, K.; Narimura, T.; Kobayashi, K.; Namatame, H.; Taniguchi, M.; Harima, H.; Shishido, H.; Ikeda, S.; Aoki, D.; Tokiwa, Y.; Haga, Y.; Ōnuki, Y. Direct observation of a quasiparticle band in $CeIrIn_5$: An angle-resolved photoemission spectroscopy study. *Phys. Rev. B* **2006**, *73*, No. 224517.
(48) Burch, K. S.; Dordevic, S. V.; Mena, F. P.; Kuzmenko, A. B.; van der Marel, D.; Sarrao, J. L.; Jeffries, J. R.; Bauer, E. D.; Maple, M. B.; Basov, D. N. Optical signatures of momentum-dependent hybridization of the local moments and conduction electrons in Kondo lattices. *Phys. Rev. B* **2007**, *75*, No. 054523.
(49) Starowicz, P.; Kurleto, R.; Goraus, J.; Schwab, H.; Szlawska, M.; Forster, F.; Szytuła, A.; Vobornik, I.; Kaczorowski, D.; Reinert, F. Evidence of momentum-dependent hybridization in Ce2Co0.8Si3.2. *Phys. Rev. B* **2014**, *89*, No. 115122.
(50) Kurleto, R.; et al. Photoemission signature of momentum-dependent hybridization in CeCoIn5. *Phys. Rev. B* **2021**, *104*, No. 125104.
(51) Ghaemi, P.; Senthil, T.; Coleman, P. Angle-dependent quasiparticle weights in correlated metals. *Phys. Rev. B* **2008**, *77*, No. 245108.
(52) Kim, H.; Choi, Y.; Lewandowski, C.; Thomson, A.; Zhang, Y.; Polski, R.; Watanabe, K.; Taniguchi, T.; Alicea, J.; Nadj-Perge, S. Evidence for unconventional superconductivity in twisted trilayer graphene. *Nature* **2022**, *606*, 494−500.
(53) Vaňo, V.; Ganguli, S. C.; Amini, M.; Yan, L.; Khosravian, M.; Chen, G.; Kezilebieke, S.; Lado, J. L.; Liljeroth, P. Evidence of Nodal Superconductivity in Monolayer 1H-TaS2 with Hidden Order Fluctuations. *Adv. Mater.* **2023**, *35*, No. 2305409.
(54) Stewart, G. R.; Fisk, Z.; Willis, J. O.; Smith, J. L. Possibility of Coexistence of Bulk Superconductivity and Spin Fluctuations in UPt_3. *Phys. Rev. Lett.* **1984**, *52*, 679−682.

https://doi.org/10.1021/acs.nanolett.4c00619
Nano Lett. 2024, 24, 4272−4278